Available online at www.sciencedirect.com
ScienceDirect
Proceedings of the Combustion Institute 31 (2007) 3261–3268
Proceedings of the Combustion Institute
www.elsevier.com/locate/proci

# On the formation of multiple rotating Pelton-like flame structures in radial microchannels with lean methane–air mixtures ☆

Sudarshan Kumar [a], Kaoru Maruta [a,*], S. Minaev [b]

[a] Institute of Fluid Science, Tohoku University, 2-1-1 Katahira, Aoba-ku, Sendai 980-8577, Japan
[b] Institute of Theoretical and Applied Mechanics, SB-RAS Novosibirsk 630090, Russia

**Abstract**

This paper reports the experimental observation of multiple Pelton-like rotating flame structures in radial microchannels with lean methane-air mixtures supplied at the center of the two closely placed circular quartz plates. The bottom quartz plate was heated with a porous burner to create a positive temperature gradient distribution along the flow direction. Stable flames were observed at a radial location for stoichiometric and rich mixtures over a wide range of operating conditions. On the other hand, for lean methane-air mixtures at $\phi = 0.67$ and channel gap of ~1–2 mm, distinct and single/multiple Pelton-like rotating flame structures were observed experimentally. These rotating flames were semi-circular in shape with a rotational speed varying from 15 to 50 Hz. Due to continuous rotation and a semi-circular flame shape; the rotating flames resemble a classical Pelton wheel. These flame structures were observed to appear over a range of velocities varying from 1.5 to 6 m/s. One, two and three rotating flames fronts appear in the domain at similar operating conditions. The effects of change in the temperature gradient and temperature profile were examined by employing a different porous burner and these modes were observed to be present for an asymmetric temperature profile. The appearance of these multiple rotating flame fronts was a function of peak temperature of the plates.


*Keywords:* Micro combustion; Radial microchannels; Pattern formation; Rotating flames

## 1. Introduction

Rotating wave patterns are widely observed in a variety of natural situations, such as propagation of electric pulses in cardiac muscles [1] and chemical reaction in premixed and non-premixed combustion systems [2–8]. The understanding of these phenomena in chemical reaction systems becomes more complex because the process is governed by fluid dynamics, chemical reaction, heat and mass transfer properties of fuel and oxidizer. Different types of flame instabilities have been reported in literature [9,10]; hydrodynamic, buoyancy driven, thermal-diffusive and viscous fingering. A prodigious amount of work has been done in the field of cellular flames [2], spiral flames [3–7] and fingering instability [8] in premixed and

☆ Supplementary data for this article can be accessed online. See Appendix A.

* Corresponding author. Fax: +81 22 217 5244.
*E-mail address:* maruta@ifs.tohoku.ac.jp (K. Maruta).

1540-7489/$ - see front matter © 2006 The Combustion Institute. Published by Elsevier Inc. All rights reserved.
doi:10.1016/j.proci.2006.07.174

non-premixed combustion systems to model and explain these phenomena.

The present work deals with experimental observation of two-dimensional flame pattern formation in radial microchannels. The interest in micro-scale combustion devices arises due to major advantages associated with these systems. These advantages include higher heat and mass transfer coefficients, higher energy densities of hydrocarbon fuels compared with those of electrochemical batteries (~20–50 times) and abatement of pollutant emissions, particularly $NO_x$, from these systems [11–16] due to their lower operating temperature. The increased heat loss due to large surface–volume-ratio adversely affects the combustion stability limits in these devices. To obtain stable combustion, thermal management, for instance, heat recirculation is a key factor for efficient operation of these devices [12,13].

Maruta et al. [14] have studied the behavior of premixed fuel-air mixtures in straight quartz tube with a 2 mm diameter and a positive temperature gradient in the flow direction. This is a simple one-dimensional configuration to study flame propagation characteristics in microchannels. In this study, a stable premixed flame was found to exist at high and extremely low mixture velocities. At moderately low velocities, three distinct, unstable flame propagation modes, (a) pulsating flame (b) flames with repetitive extinction and ignition (FREI) and (c) a combination of pulsating and FREI modes were observed. Linear stability analysis also predicts the existence of different stable and unstable propagation modes over a range of velocities and equivalence ratios [15].

In the present work, experimental observations of dynamic and unsteady flame front movements in radial microchannels are presented. This work is essentially an extension of previous 1-D work [14] to two-dimensions to understand flame propagation characteristics in expanded dimensions. In a real practical application, the combustion room is two or three-dimensional [16] and fuel–air mixture is subjected to both temperature and flow divergence depending upon the combustion room configuration. Therefore, to understand the peculiarities of the combustion of methane–air mixtures in the extended dimensions, the present configuration of a radial microchannel was chosen in which a combustible mixture was subjected to combined positive temperature gradient and negative velocity gradients.

## 2. Experimental setup

A schematic diagram of the experimental setup is shown in Fig. 1. Two quartz plates were maintained parallel to each other within ±0.1° accuracy with the help of a level-indicator. To simulate

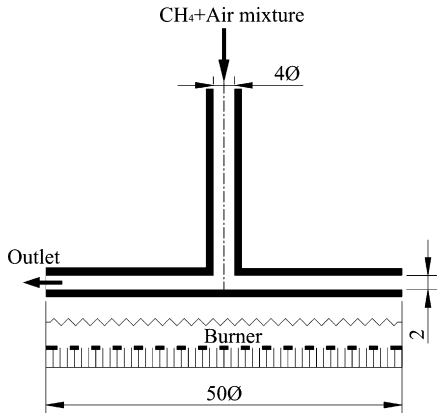


Fig. 1. Experimental setup.

the heat recirculation process, a 1 mm thick quartz (bottom) plate was placed 10 mm above the porous burner and heated continuously. This helped to create positive temperature gradient conditions in the walls, when mixture was injected at the center through a 4 mm diameter mixture delivery tube. A constant heating rate was used during all the experimental investigations to exclude the effect of temperature distribution variation with heating rate on the observed flame patterns. The temperature profile along the inner side of the bottom plates was measured in the case of airflow with a 300 μm K-type thermocouple. During the wall temperature measurements, airflow through the mixture delivery tube at a velocity of 4 m/s was supplied to examine its effect on the temperature profile. Curve $T_1$ in Fig. 2 shows the measured temperature profile on the inner side of the bottom plate ($T_2$ profile is discussed later). The top plate is heated due to convection and radiation from the bottom plate, and measured temperature distribution is similar to that of bottom plate with a slightly lower temperature (~20–50 K). The measured temperature profile of the present experiments is similar to that of Maruta et al. [14] with the lowest measured temperature

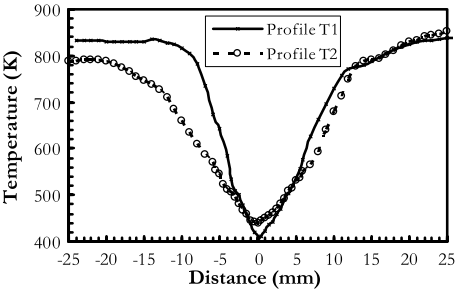


Fig. 2. Measured temperature profiles of the bottom plate. $T_1$ = symmetric, $T_2$ = asymmetric.

of 410 K at the center and the highest temperature of 830 K at a radius of 13 mm. The highest measured temperature along with the temperature gradient (~32 K/mm) can be used as representative parameters for the present study. The delivery tube was cooled to maintain the upstream temperature of the incoming mixture. Methane gas with 99.99% purity was used as fuel. Electric mass flow controllers were used to precisely monitor the mass flow rates of methane and air within an accuracy of ±1%.

Preliminary observations were carried out with a normal CCD video camera. Due to the highly unsteady nature of the combustion process, normal movie recording was carried out with a high-speed video camera, "FASTCAM-NEO-Photron." High-speed video recording was carried out from a sideways angular position of approximately 30° because the presence of the vertical mixture delivery tube restricted the top view of the quartz plates. The picture resolution was $512 \times 512$ pixels over a range of the image capturing speeds varying from 30 to 20,000 Hz. Flame images were recorded at a rate of 1000 frames/second with a shutter speed of 1/2000 s. During each run, 2048 frames were recorded and images were further analyzed with image processing software PFV-ver.2.2.2.1 [17].

## 3. Results and discussion

### 3.1. Preliminary observations

Parametric studies were carried out to distinguish the different flame propagation modes observed in the present experiments. The parameters investigated were mixture equivalence ratio, plate separation distance and mixture velocity. The typical mixture velocity through the mixture delivery tube was varied in the range of 1.5–7 m/s. The bottom plate was heated with a porous burner and air supply through mixture delivery tube was continued to obtain positive temperature gradient in the flow direction. Once the temperature of the plates achieved steady state, the fuel supply was initiated along with continued air supply through the delivery tube. The distance between two quartz plates was 5 mm at the start of the experiment. The plate separation distance was reduced by 0.25 mm in each step with a micrometer traverse (0.05-mm resolution). The following schemes were used to categorize the different flame front propagation modes observed during the experimental studies:

1. Flame propagation modes with stable flame front characteristics were assigned to group A (A-stable, A-broken).
2. Flame propagation modes with unstable behaviors were assigned to group B (B-Pelton).
3. All other modes were assigned to groups C and D.

Preliminary observations carried out with a CCD video camera are shown in Fig. 3. Stable and unstable flame propagation modes were observed over a range of operating conditions. In combustion regime A-stable, a stable flame front was located at a radial location, as shown in Fig. 3a. The radial location of the flame front is a function of mixture velocity, equivalence ratio and plate separation distance. Figure 3b shows the observation of an unstable flame propagation mode. At $\phi = 0.67$ and $d = 1.75$ mm, a B-Pelton unstable flame propagation mode was observed for a range of mixture velocities varying from 1.5–6.0 m/s. More details on this flame propagation mode are presented in the following sections. Figure 3c shows the A-broken combustion mode. This flame propagation mode generally appeared at very small plate separation distances. Due to decrease in channel width, the flame quenched at one point in the domain and this extinction spot propagated in the angular direction. Figure 3d shows the combustion regime C, which was observed at high velocity and large plate separation distance ($\geqslant 4$ mm). In this mode, an asymmetrical and steady flame with weak visibility was observed. In group D, a stable flame front was observed at the mixture delivery tube exit. The C and D flame propagation modes were not pursued further because flame stabilizes at the outlet and inlet for high and low mixture velocity conditions respectively and could be equated with flame flashback and flame blowout limits.

A brief summary of experimental conditions for various stable and unstable flame propagation modes is given in Table 1. A-stable was observed at $\phi = 0.85$, $U = 3$ m/s and $d = 0.25$–5.0 mm.

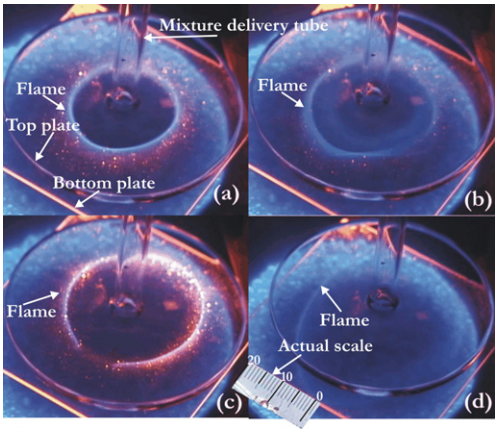


Fig. 3. Classification of different flame-fronts observed with a CCD video camera. (a) A-stable, (b) B-regime, (c) A-Broken, and (d) C-regime.

Table 1
Brief summary of experimental conditions for different flame propagation modes

| Propagation mode | $\phi$ | $U$ (m/s) | $d$ (mm) |
|---|---|---|---|
| A-stable | 0.85 | 3.0 | 0.25–5 |
| A-broken | 0.67 | 3.5 | 0.50 |
| C-mode | 0.67 | 7.0 | 5.0 |
| B-Pelton | 0.67 | 1.5–6 | 1.75 |

A-broken mode was observed at $\phi = 0.67$ and a short plate separation distance. The effect of mixture equivalence ratio on flame stability was investigated by changing the mixture equivalence ratio from 0.85 to 0.67. The stable flame propagation mode disappeared with the decrease in the equivalence ratio and different unsteady flame propagation modes appeared. B-Pelton, an unsteady flame propagation mode was observed at $\phi = 0.67$ or lower equivalence ratios and over a wide range of mixture velocities. Kumar et al. [18] have presented a detailed description of these stable and unstable flame propagation modes. Therefore, the present paper is concerned with the appearance of multiple rotating Pelton-like flames observed with lean methane-air mixtures at $\phi = 0.67$. A detailed description is given in the following sections.

### 3.2. Regime diagram for Pelton-like rotating flames

To obtain a regime diagram, the plate separation distance was fixed at 1.75 mm and $\phi = 0.67$. The mixture velocity was varied gradually and at times randomly over a range of 1.5–6 m/s to observe the various modes of the propagating flame fronts. Figure 4 shows the regime diagram for Pelton-like rotating flames. A single Pelton flame (one Pelton-flame front) is observed over the whole range of mixture velocities. The domain of existence for double Pelton flame (two Pelton-flame fronts) narrows towards the center of the diagram and triple Pelton flame (three Pelton-flame fronts) is observed only in a very small velocity range of 3.0–3.5 m/s. An interesting point is the existence of multiple modes for a particular velocity condition. For instance, in the mixture velocity range of 3.0–3.5 m/s, the various flame propagation modes with one/two/three flame fronts are observed fortuitously at the same conditions. These modes with single/double/triple Pelton-like flames were observed to occur by randomly changing the mixture velocity.

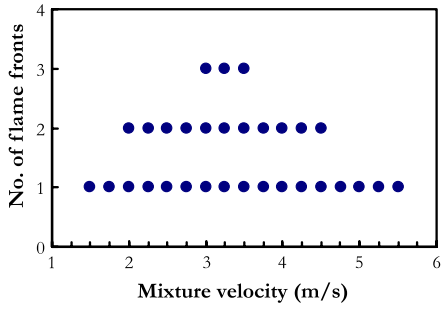


Fig. 4. Number of Pelton-like flames with mixture velocity variation.

### 3.3. Single Pelton flame propagation mode

Figure 5 shows a single Pelton flame pattern observed in the narrow gap between two plates, (see Supplementary material). These pictures were recorded at $\phi = 0.67$, $U = 1.5$ m/s and $d = 1.75$ mm. These frames show the position of propagating flame front after 4-ms time intervals. The rotational speed of this flame front was approximately 40 Hz. In this regime, one flame front, nearly semicircular in shape, was observed, which revolves around the center of the plates in a cyclic motion. This semicircular-shaped flame front coupled with rotational motion resembles a classical Pelton wheel. A similar hemispherical propagating flame in a tube was experimentally observed by Kim et al. [19] at low pressure and near extinction limit conditions.

The background flame of the porous burner imparted some noise for direct video recording and resulted in poor visualization. Therefore, to present a better view of the observed flame patterns, the heating burner was switched off during the high-speed video recording. It is assumed that the flame front pattern remained unaffected for a certain period of time. The pictures shown in the present paper were taken within first 80-ms after the heating burner had been switching off. This time period is very small compared to the change in observed phenomena which occurred ~800–2000 ms after the heating burner had been switching off.

The radial location of the propagating flame front depends on the mixture velocity. This flame front was observed to rotate in both clockwise and counterclockwise directions. This flame rotation in both clockwise and counterclockwise directions seemed to occur with equal probability. The onset of the rotational direction in this flame propagation mode is not clear at this moment; however, it could be possible that the direction of rotation is triggered through an internal or external disturbance at a particular location, which determines the rotational direction for the flame front. This is an example of a system in neutral equilibrium with a tendency to rotate either clockwise or counterclockwise depending on the direction of initial perturbation. A similar rotational behavior of spiral flames propagating in a tube was observed by Pearlman and Ronney [3] and Pearlman [4],

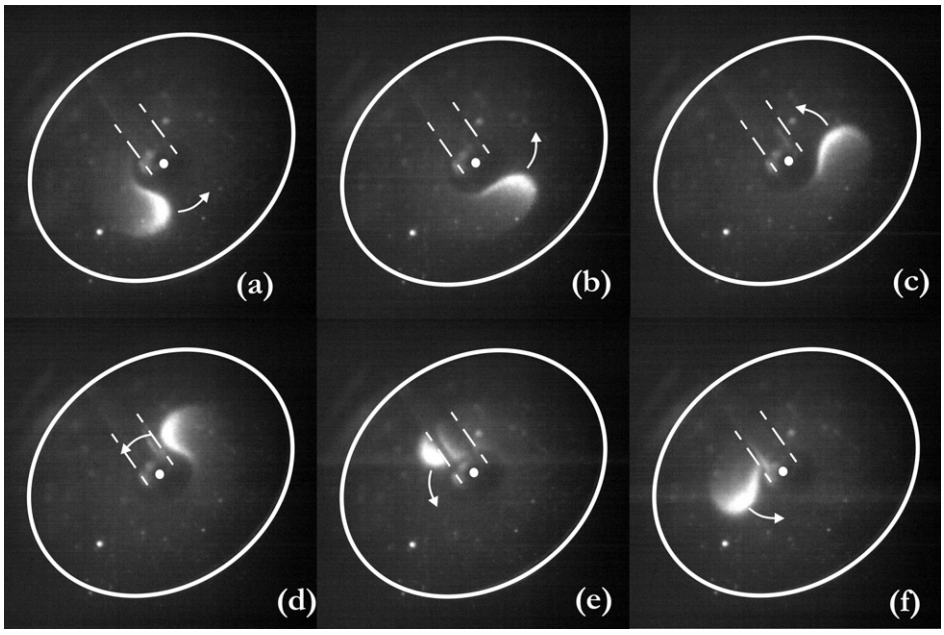


Fig. 5. Single Pelton-flame propagation mode.

where these spiral flames patterns were observed to rotate in both directions with equal probability.

### 3.4. Double Pelton flame propagation mode

In this flame propagation mode, two propagating flame fronts were observed. These flame fronts were separated by 180° and located opposite to each other in the domain. These flames were semi-circular in shape and observed to rotate in a cyclic motion around the center of the plates. Figure 6 shows the motion of these flame fronts in clockwise direction (see movie in Supplementary material). Each image shows the position of flame front after 2-ms time intervals. In this figure, a half rotational cycle is shown (the other half cycle motion is identical); and these flames rotated at ~32 Hz. The two propagating flames were observed to rotate in both clockwise and counterclockwise directions.

### 3.5. Triple Pelton-flame propagation mode

In this flame propagation mode, three flame fronts existed in the experimental domain simultaneously. These flame fronts rotated around the center of the plates with a cyclic motion. They were separated by approximately 120° from each other as shown in Fig. 7 (see Supplementary material). The frames show the flame front positions at every 2-ms time intervals; and they rotate in counterclockwise direction. One-third of the rotational cycle is shown in this figure and these flames rotate at a rate of ~28 Hz. These propagating flames are also observed to rotate in both clockwise and anti-clockwise directions.

### 3.6. Effect of temperature gradient

To investigate the effect of temperature profile on these flame propagation modes, two different porous burners were used. The temperature profiles $T_1$ and $T_2$ shown in Fig. 2 were obtained using 40- and 20-μm sized porous burners, respectively. The characteristics of single Pelton mode were investigated with $T_1$ and $T_2$ temperature profile conditions at 3.0 and 4.0 m/s mixture velocities. Figure 8 shows the trajectories followed by the traveling flame front with temperature profiles $T_1$ and $T_2$ at 3.0 m/s mixture velocity. These trajectories were obtained by tracking a point on the rotating flame front for one complete rotation and the errors in the estimation of flame trajectory using this method are expected to be within a few percent. For $T_1$, the single flame front followed a nearly circular motion in the domain as indicated by a dashed circle drawn in the figure. For $T_2$, the motion of the propagating flame front stretches in the domain towards the low temperature side when compared to $T_1$. Similar behavior of the propagating flame fronts is observed at 4 m/s mixture velocity. The trajectory of the propagating flame front shifted towards left due to lower wall temperature on the left side of curve $T_2$ in Fig. 2, resulting in asymmetric rotational behavior. The

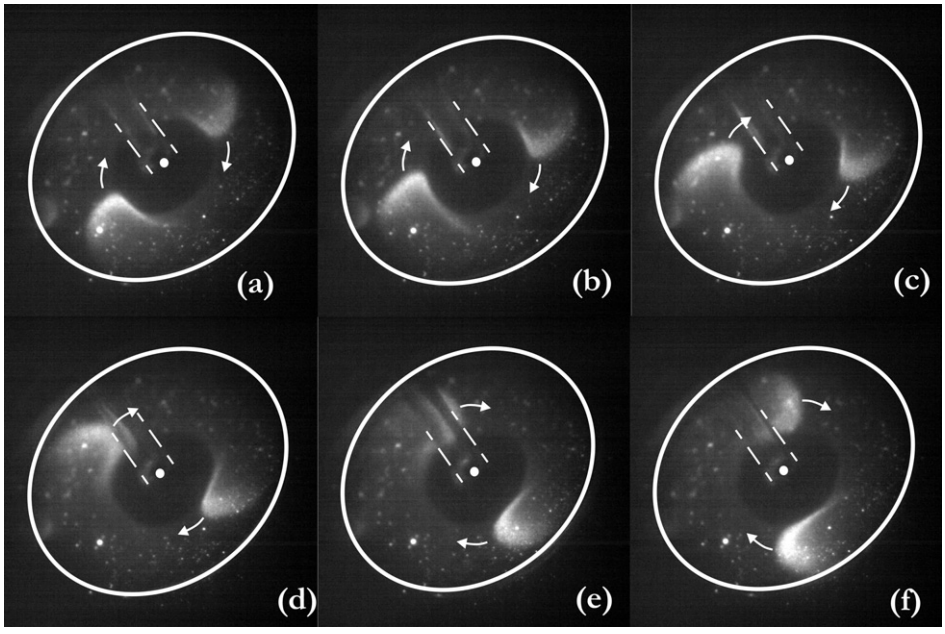


Fig. 6. Double Pelton-flame propagation mode.

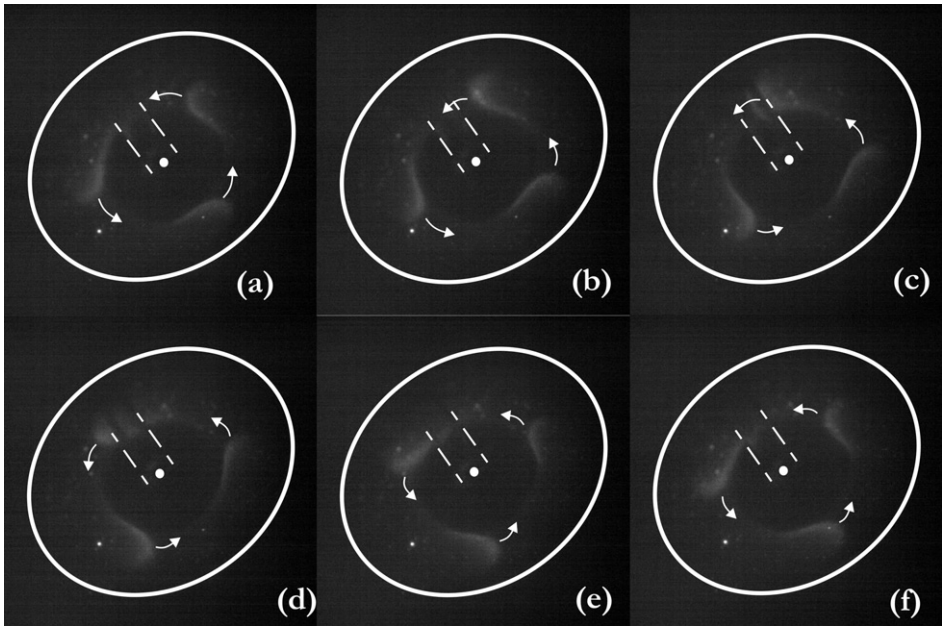


Fig. 7. Triple Pelton-flame propagation mode.

change in the temperature profile also affected the rotational speed of the flame front. The rotation speed changed from 24 Hz ($T_1$) to 21 Hz ($T_2$) at a mixture velocity of 3.0 m/s. A similar reduction from 22 to 17 Hz in the rotational speed was observed at a velocity of 4.0 m/s. The rotational frequency of these flames decreased due to an increase in the circumference of these propagating flames for $T_2$ temperature profile. However, it is noteworthy that the change in temperature profile did not affect the appearance of the phenomena. The appearance of these Pelton-like rotating

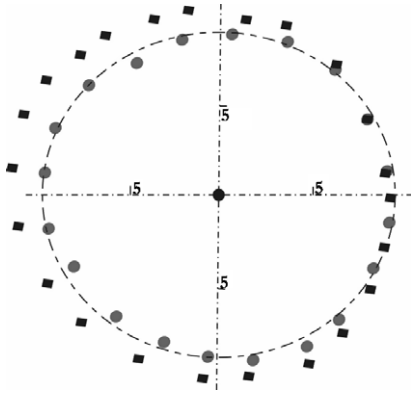

Fig. 8. Effect of temperature profile on flame-front trajectory. (●) $T_1$ temperature profile; (■) $T_2$ temperature profile.

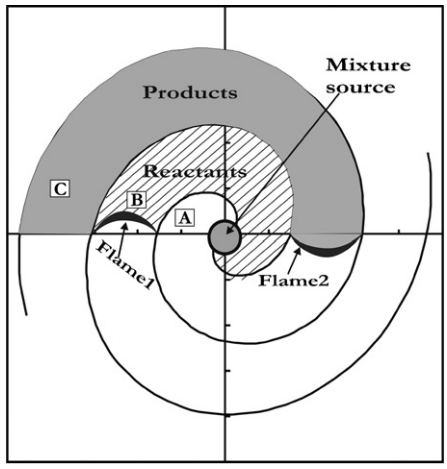


Fig. 9. Schematic diagram to explain the appearance of multiple Pelton-like flame modes.

flames seemed to be dependent on the peak plate temperature, and the temperature gradient/profile only affected the flame trajectory.

## 4. Discussion

The mechanism of multiple Pelton-like flames is remains unclear, and thus an effort has been made to propose a possible propagation mechanism and explain these interesting observations. Figure 9 shows a schematic to explain the observation of rotating Pelton flame behavior which results from the coupling of a radial flow emanating from a cylindrical source at the center without rotational flow. Two spirals are assumed (one/three can also be assumed to explain single/triple Peltons) to be generated at the cylindrical source to explain the formation of multiple Pelton flames. It has been theoretically shown that a radial flow can generate rotating flame patterns [18] and flow rotation is not an important condition. However, due to momentum imbalance, flow rotation can be induced by rotating flame structures, although the actual mechanism is unclear at present. The fresh reactants issued from the cylindrical source follow a spiral motion and two Pelton flames (Flame-1 and Flame-2 in Fig. 9) located opposite each other are formed at a particular radial location. These flames continuously rotate around the mixture source at a certain frequency. The existence and propagation of Flame-1 can be explained as being due to the existence of an interface of combustion products emanating from Flame-2 (zone-C) and fresh reactants (zone-B) of Flame-1. Similar existence of an interface between combustion products and fresh reactants is also predicted for quasi-steady spiral flames [6]. The amount of dilution at the interface surface determines the outer radius and shape of Flame-1. With the increase in the number of flame fronts (single → double → triple), the time available for dilution decreases sharply and this perhaps affects the flame front shape to a certain extent. For instance, change in the outer shape of the Pelton flames with the increase in the number of flame fronts can be noticed from Figs. 5–7. On the inner side of the flame front, there is an interface of fresh reactants between zone-A and zone-B. Flame extinction occurs at a particular radial location and flame does not propagate into zone-A due to the following reasons. (1) The existence of a positive temperature gradient in radial direction (Fig. 2) results in flame stabilization at a particular radial location, where wall temperature is sufficiently high to stabilize the flame. (2) The flow velocity decreases linearly in the radial direction. Therefore, the residence time of reactants is much shorter in zone-A due to higher flow velocity compared with zone-B. Therefore, the flame front does not propagate towards zone-A due to adverse conditions of low wall temperature and high flow velocity in zone-A. It is difficult to explain the appearance of multiple (two/three) Pelton flames within an interval of gas velocities. It is obvious that the number of observed flame fronts increases with mixture velocities because two or three Peltons consume large amounts of fresh mixture than a single one, therefore they appear at higher mixture velocities. However, it is hard to explain the decrease in the number of Pelton flames with velocity at higher flow rates.

## 5. Conclusions

We have herein reported the formation of multiple Pelton-like flames in radial microchannels with lean methane-air mixtures. These rotating semi-circular shaped flames resemble the classical

Pelton wheel geometrically; therefore, these flames are called as Pelton flames. Single/double/triple Pelton flames were observed over a range of velocities varying from 1.5–6 m/s. A possible mechanism is proposed for these rotating Pelton-like flames. The radial flow from the cylindrical source leads to the formation of spirals and an interface of combustion products and fresh reactants exists at the outer side of the flame. On the inner side, flame extinction occurs due to adverse conditions of temperature and velocity gradients near the center. The rotational speed of these Pelton flames varies from 15 to 50 Hz and is observed to decrease with a decrease in the wall temperature. The change in the temperature profile does not affect the appearance of Pelton flames. However, these flames are more dependent on the peak temperature of wall and the temperature gradient only affects the flame trajectory. These rotating flames show potential for use as heat sources for various future applications, for instance, thermal pulses in a two-dimensional domain and thermoelectric converters.

## Appendix A. Supplementary data

Supplementary data associated with this article can be found in the online version at doi:10.1016/j.proci.2006.07.174.

## References

[1] J.M. Davidenko, A.V. Pertsov, R. Salomonsz, W. Baxter, J. Jalife, *Nature* 355 (1992) 349–351.
[2] M. Gorman, M. el-Hamdi, B. Pearson, *Phys. Rev. Lett.* 76 (1996) 228–231.
[3] H.G. Pearlman, P.D. Ronney, *Phys. Fluids* 6 (1994) 4009–4018.
[4] H.G. Pearlman, *Combust. Flame* 109 (1997) 382–398.
[5] V. Nayagam, F.A. Williams, *Phys. Rev. Lett.* 84 (2000) 479–482.
[6] S. Kumar, K. Maruta, S.S. Minaev, R. Fursenko, *Phys. Fluids* (2006) under review.
[7] V. Panfilov, A. Bayliss, B.J. Matkowsky, *Appl. Math. Lett.* 16 (2003) 131–135.
[8] M.L. Frankel, G.I. Sivashinsky, *Phys. Rev. E* 52 (1995) 6154–6158.
[9] G.I. Sivashinsky, *Annu. Rev. Fluid Mech.* 15 (1983) 179–199.
[10] F.A. Williams, *Combustion Theory*, Benjamin Cummings, 1985, p.341.
[11] A.C. Fernadrz-Pello, *Proc. Combust. Inst.* 29 (2002) 883–899.
[12] P.D. Ronney, *Combust. Flame* 135 (2003) 421–439.
[13] S.A. Lloyd, F.J. Weinberg, *Nature* 251 (1974) 47–49.
[14] K. Maruta, T. Kataoka, N.I. Kim, S. Minaev, R. Fursenko, *Proc. Combust. Inst.* 30 (2005) 2429–2436.
[15] K. Maruta, J.K. Parc, K.C. Oh, T. Fujimori, S.S. Minaev, R.V. Fursenko, *Combust. Explos. Shock Waves* 40 (2004) 516–523.
[16] N.I. Kim, S. Kato, T. Kataoka, T. Yokomori, S. Maruyama, T. Fujimori, et al., *Combust. Flame* 141 (2005) 229–240.
[17] Photron Fastcam Viewer PFV-ver2.2.2.1 (2001), available at <http://www.photron.com/>.
[18] S. Kumar, S. Minaev, R. Fursenko, A. Mukhopadhyay, K. Maruta, Combust. Flame (2005), under review.
[19] N.I. Kim, T. Kataoka, S. Maruyama, K. Maruta, *Combust. Flame* 141 (2005) 78–88.